CORE
Metadata, citation and similar papers at core.ac.uk
Provided by Universidade do Minho: RepositoriUM

Optical properties of AlN_xO_y thin films deposited by DC magnetron sputtering

J. Borges*[a], E. Alves[b] F. Vaz[a], L. Marques[a]
[a]Centro de Física, Universidade do Minho, 4710-057 Braga, Portugal
[b]Departamento de Física, Instituto Tecnológico Nuclear, E.N. 10, 2686-953 Sacavém, Portugal

ABSTRACT

The aluminium oxynitride system offers the possibility to obtain a wide range of optical responses, by combining metallic aluminium, aluminium oxide and aluminium nitride properties, and thus opening a significant number of possible applications. The main purpose of the present work is to study the variation of the optical properties of AlN_xO_y thin films as a function of their composition (by varying both x and y coefficients), and the correspondent changes in their morphology and structure. The films were deposited by DC reactive magnetron sputtering, with the discharge parameters monitored during the deposition in order to control the chemical composition. The measurements reveal a smooth change of films Reflectance/Transmittance as a function of the concentration ratio of non metallic elements (O+N) to metallic Al, thus revealing the possibility to tailor the films optical properties according to the application envisaged.

Keywords: Aluminium oxynitride, DC reactive magnetron sputtering, optical properties

1. INTRODUCTION

Metallic aluminium (Al), aluminium nitride (AlN) and aluminium oxide (Al_2O_3) are three well studied materials that are used in different technological fields and applied in a wide variety of different devices.

*joelborges@fisica.uminho.pt

Aluminium is a metallic material used in several applications including as a standard in reflectance measurements due to its high reflectance (85% to 98% between 250 nm to 2500 nm). Moreover these high reflectance values allow the use of aluminium also as mirror and in optical coatings. The dielectric function of polycrystalline aluminium is normally described by a Drude model for intraband transitions (the bulk plasmon frequency is approximately 15 eV) and two strong interband transitions at 0.5 eV and 1.5 eV [1, 2].

Aluminium nitride, AlN, in known to be as a semiconductor with a large bandgap [3] (6.2 eV) in its more stable *wurtzite* crystalline structure [4, 5] and reveals a refractive index of about 2.1-2.2 in the visible range [1, 6]. Exhibits high electrical resistivity, high hardness and it is also a piezoelectric material [7]. AlN is commonly used in fabrication of optical sensors in the ultraviolet-visible region, light emitting diodes (LEDs) with one of the shortest emission wavelength reported (210 nm) [8]; and several types of microelectronic-related applications [9-12].

Aluminium oxide, or alumina Al_2O_3, is one of the well-known corrosion resistant materials, even at high temperatures [13-15]. Alumina reveals also a large bandgap (9 eV) and possesses a relatively low refractive index in the order of about 1.7-1.8 in the visible range[1, 16]. This last characteristic enables this material to be used as protective film for metal reflectors, dark mirrors, and in metal-oxide-semiconductor devices [17].

The joining of the properties of these three base materials Al, Al_2O_3 and AlN, by developing a mixed Al-N-O system, allows combining some of the most relevant advantages of the base systems, by tailoring the concentrations of the three elements, according to desired application. In spite of this possible combination of properties form by each of the base systems, the use of aluminium oxynitride (AlN_xO_y) films is still very restrict, despite some known examples as protective coating against wear, diffusion and corrosion, optoelectronics, microelectronics [18] and as dielectric in multilayer capacitors with higher energy density and wide temperature properties.

Another important fact is that aluminium oxynitride (AlNO) can crystallize in a cubic *spinel* structure which is known to be a ceramic material with high strength and hardness. It can be four times harder than SiO_2 glass and transparent from UV to NIR wavelengths [19, 20].

Taking the above as a starting point, the major concern of this work is to study the different optical responses of AlN_xO_y thin films, by varying the N to O ratio and the consequent variations in the films morphological and structural features. The films are deposited using DC reactive magnetron sputtering, varying the discharge parameters in order to tailor the composition of the films.

2. EXPERIMENTAL DETAILS

The thin films were deposited by reactive DC magnetron sputtering, in a laboratory-sized deposition system. The films were prepared with the substrate holder positioned at 70 mm from the target in a rotation mode-type (9 r.p.m.). A DC current density of 75 $A.m^{-2}$ was used on the aluminium target (99.6% purity).

The substrates (glass and monocrystalline silicon wafers with (100) orientation) were grounded and kept at a constant temperature of approximately 373 K during the deposition (using a Joule effect resistor) and were subjected, before the deposition, to an etching process, using pure argon with a partial pressure of 0.3 Pa and a pulsed current of 0.6 A (T_{on} = 1536 ns and f = 200kHz) for 900 s. The temperature evolution of the coated substrates was monitored with a thermocouple placed close to the surface of the substrate holder.

For the preparation of the films, the aluminium target (200x100x6 mm^3) was sputtered using a gas atmosphere composed of argon (working gas, at a constant partial pressure of 0.3 Pa), and a mixed nitrogen and oxygen reactive mixture with a constant N_2/O_2 ratio of 17/3. The discharge parameters: target potential and current, gas pressure, argon flow and reactive gas flow, were monitored using a Agilent 34970A Data Acquisition system. The atomic composition of the as-deposited samples was measured by Rutherford Backscattering Spectroscopy (RBS), using 1.4 and 1.75 MeV proton beams and a 2 MeV He^{4+} beam. Two different detectors were used at scattering angles of 140° and 180°, and experiments were made at tilt angles 0° and 30°. Composition profiles for the as-deposited samples were determined using the software NDF [21].

The structure and the phase distribution of the coatings were analyzed by X-ray diffraction (XRD), using Cu-Kα radiation operating in a Bragg–Brentano configuration.

Scanning electron microscopy (SEM) was made to determine the thickness of the films and to study its morphology.

The optical reflectance and transmittance of the samples were measured with a Shimadzu UV-3101 PC UV-Vis-NIR, using an integrating sphere of 60 mm (inner diameter) in both measurements.

3. RESULTS AND DISCUSSION

3.1 Chemical composition

The chemical composition of the AlN_xO_y films, obtained from RBS spectra, is reported in Table 1, along with the thickness of each sample obtained by scanning electron microscopy. The table shows the variation of the atomic concentration (at. %) of the film's elements, but also the correspondent concentration ratios of non metallic/metallic elements, C_N/C_{Al}, C_O/C_{Al} and C_{N+O}/C_{Al}). According to the obtained results, one can distinguish two main groups of samples, where the films reveal quite different characteristic features of both metallic and insulating-type ones. The first zone (indexed hereafter as zone M), consists of opaque metallic-like films, with very low ratios of non-metallic over metallic elements ($C_N/C_{Al} \leq 0.06$) and revealing a typical columnar-like growth.

A second major group of samples (which will be labeled hereafter as Zone C) reveals over-stoichiometric AlN_xO_y compounds, with very similar C_O/C_{Al} concentration atomic ratios (about 1.5), and residual values of nitrogen. The composition analysis of these films provides evidence of aluminum oxide (Al_2O_3) type films. The films are dense and semi-transparent, with interference like colorations and featureless-type of growth. All these characteristics are coherent with oxide-like films.

Between these two main zones of films, one can distinguish a transition zone, zone T, were the non-metallic over aluminium ratios are in between metallic and oxide-like films ($0.18 \leq C_{N+O}/C_{Al} \leq 0.85$), inducing the possibility to prepare sub-stoichiometric AlN_xO_y-type films. The films ascribed to this transition zone are opaque, with dark grey color tones, revealing an unusual cauliflower-type of growth.

Sample	Partial pressure of reactive gas (N_2+O_2)	C_{Al} /at.%	C_O / at.%	C_N /at.%	C_O/C_{Al}	C_N/C_{Al}	C_{N+O}/C_{Al}	Type of growth	Thickness /µm
S #1	0.00	100	0	0.0	0.0	0.0	0.0		3.26
S #2	0.006	96	0	5	0	0.05	0.05	Columnar	2.17
S #3	0.016	94	5	1	0.05	0.01	0.06		2.04
S #4	0.030	85	10	5	0.12	0.06	0.18		5.67
S #5	0.034	71	18	11	0.25	0.16	0.41		2.89
S #6	0.044	61	26	13	0.42	0.22	0.64	Cauliflower	2.04
S #7	0.050	61	21	18	0.34	0.30	0.65		3.26
S #8	0.054	54	19	27	0.34	0.50	0.85		2.96
S #9	0.056	39	61	0	1.58	0.01	1.59		0.40
S #10	0.060	40	60	0	1.50	0.00	1.50	Dense, featureless	0.08
S #11	0.060	40	60	0	1.50	0.00	1.50		0.23

Table 1 - Chemical composition and thickness of the deposited coatings.

3.2 Structure

Figure 1 shows the X-ray diffraction patterns for representative AlN_xO_y films indexed to zones M and T. The films ascribed to zone C (not represented) are amorphous.

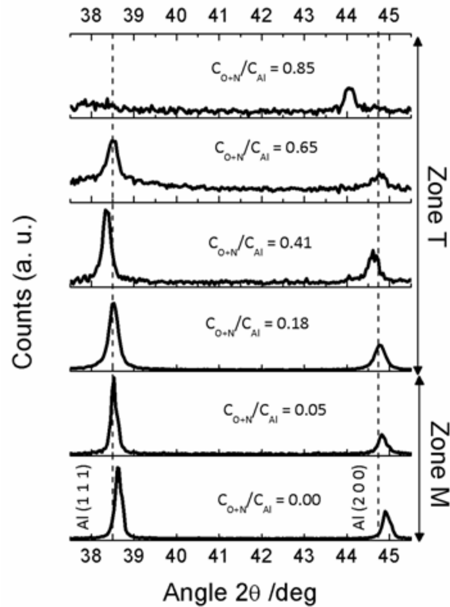

Figure 1 – X-ray patterns of the deposited AlN_xO_y thin films.

The *quasi*-pure aluminium film exhibits the characteristic face-centered cubic (fcc) structure of (bulk) aluminium [22]. The two diffraction peaks represented in fig. 1 for each sample correspond to (111) and (200) planes of such fcc structure, with a (111) preferential orientation of the grains. This preferred orientation is to be expected in a fcc structure since the coarsening of the grains during coalescence induces the growth of islands with the densest planes, (111) in this particular case, as the microstructure of the film is evolving [23]. The increase of oxygen and nitrogen content in zone T is followed by a gradual amorphization. Therefore more disorder is expected to occur in these films, since the increase of oxygen and nitrogen promoted by the increase of the reactive gas partial pressure induces structural defects such as interstitials, vacancies and some residual doping elements in the structure of the aluminium, which reduces the possibility of crystallization. Further detailed analysis of

the structural features, including grain size variations and lattice parameters change, can be found elsewhere [24].

3.3 Optical properties

To study the optical properties of these coatings, some optical measurements (reflectance and transmittance) were performed. Figure 2 shows the absolute reflectance of the opaque samples in the range of 300 nm to 2500 nm. A *STAN-SSH High-reflectivity Specular Reflectance Standard* was used as standard for high reflective samples and Barium Sulfate for the low reflective ones. The metallic-like samples, S #1 and S #2, have the typical reflectance of polycrystalline aluminium, with a strong interband transition at approximately 815 nm. Sample S #3 reveals a reflectance spectra very distinct from the previous samples, exhibiting a marked decrease of the reflectance in the IR range until a minimum of reflectance is reached (25%), for a wavelength of approximately 815 nm (the wavelength of the interband transition of aluminium), followed by increase of reflectance in the visible and UV range. The films from Zone T reveal very interesting features, exhibiting very low values of reflectance (below 10%) and almost constant values all over the spectral range.

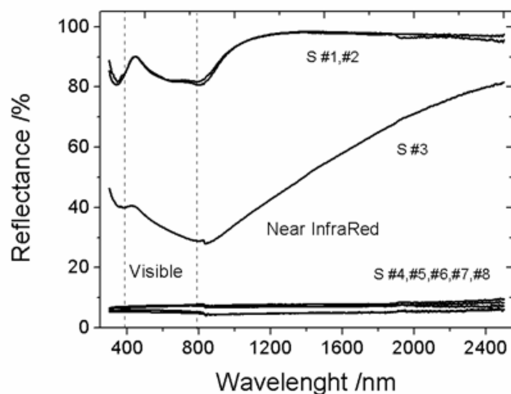

Figure 2 –Reflectance spectra from zone M and zone T films, as a function of the wavelength.

Figure 3 presents the reflectance spectrum of sample S #1, fitted using the SCOUT software (*W. Theiss soft- and hardware*) assuming a Drude model, Kim extended oscillator model and a OJL interband transition model. The Drude plasma energy given by the fit is approximately 11.3 eV, the interband transition energy of 1.3 eV. One can also find two oscillators with resonance frequencies of 3.7 eV and 2.1 eV.

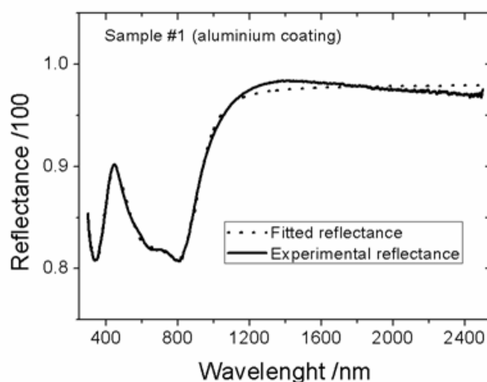

Figure 3 – Experimental and fitted reflectance of the aluminium coating (sample S #1).

Figure 4 shows the transmittance of the amorphous alumina coatings deposited on glass. One can observe that the transmittance slightly decreases as the thickness of the samples increases, due to the higher absorption of the films. Despite this fact, the transmittance is higher than 80% for all the samples. Furthermore one can observe the appearance of several interference fringes for sample S #9, consistent with the higher thickness of this sample. For the case of sample S #11, the reflectance spectrum was also measured and the refractive index extracted using the SCOUT software, simulating both experimental spectra (reflectance and transmittance). In the fitting process, a Cauchy model [25] was assumed to be able to describe the thin film optical properties. The fitting results are shown in fig. 5(a-b), where one can observe a good agreement between the simulated and experimental spectra. Figure 5(b) shows the variation of the simulated refractive index of this coating as a function of the wavelength, which is in accordance with the Al_2O_3 refractive index in the literature[1].

The measurements reveal a smooth change of films Reflectance/Transmittance as a function of the concentration ratio of non metallic elements (O+N) to metallic Al, thus opening the possibility to tailor the films optical properties according to the application envisaged.

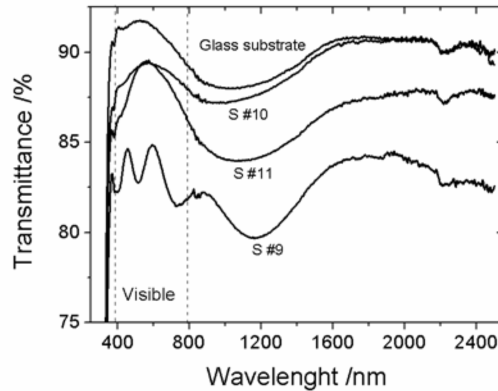

Figure 4 –Transmittance spectra from zone C (Al_2O_3 films), as a function of the wavelength.

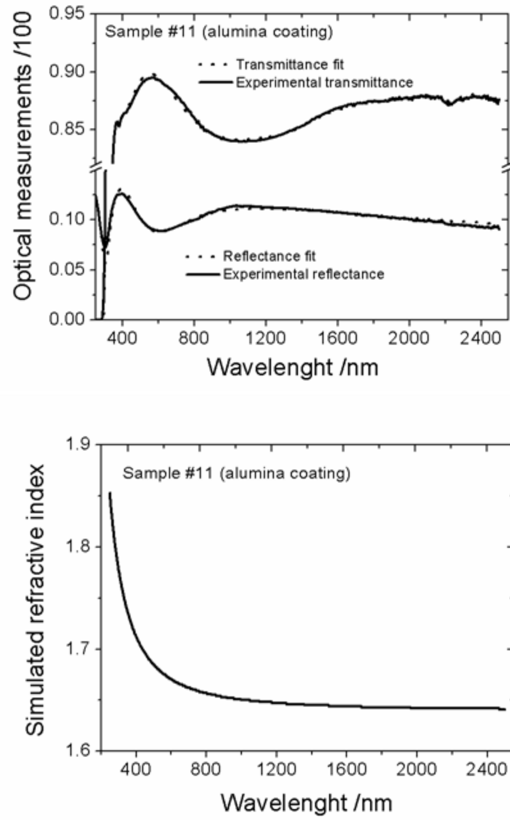

Figure 5 – (a) experimental and fitted reflectance and transmittance of the sample S #11 and (b) simulated refractive index.

4. CONCLUSIONS

AlN_xO_y thin films were deposited by DC reactive magnetron sputtering, using an aluminium target and a mixture of nitrogen and oxygen (17:3) as reactive gas. Varying the pressure of reactive gas, coatings with different chemical compositions and distinct optical properties were obtained. Three different types of coatings can be identified. A first set of samples (Zone M) exhibiting very high reflectance and metallic-like colors. A second set of samples follows with dark grey colors and very low reflectances in all spectral range. Finally a last group of samples with semi transparency characteristics with interference like colorations. It is thus possible to tune the films optical properties according to the application envisaged, by simply changing reactive gas flow during processing.

5. REFERENCES

[1] Palik, E. D., [Handbook of Optical Constants of Solids] Elsevier.

[2] Smith, D. Y., and Segall, B., "Intraband and interband processes in the infrared spectrum of metallic aluminum," Physical Review B, 34(8), 5191 (1986).

[3] Venkataraj, S., Severin, D., Drese, R. *et al.*, "Structural, optical and mechanical properties of aluminium nitride films prepared by reactive DC magnetron sputtering," Thin Solid Films, 502(1-2), 235-239 (2006).

[4] Vispute, R. D., Narayan, J., and Budai, J. D., "High quality optoelectronic grade epitaxial AlN films on [alpha]-Al2O3, Si and 6H-SiC by pulsed laser deposition," Thin Solid Films, 299(1-2), 94-103 (1997).

[5] Wang, J., Wang, W. L., Ding, P. D. *et al.*, "Synthesis of cubic aluminum nitride by carbothermal nitridation reaction," Diamond and Related Materials, 8(7), 1342-1344 (1999).

[6] Zhao, S. X., and Wackelgard, E., "The optical properties of sputtered composite of Al-AlN," Solar Energy Materials and Solar Cells, 90(13), 1861-1874 (2006).

[7] Mortet, V., Nesladek, M., Haenen, K. *et al.*, "Physical properties of polycrystalline aluminium nitride films deposited by magnetron sputtering," Diamond and Related Materials, 13(4-8), 1120-1124 (2004).

[8] Taniyasu, Y., Kasu, M., and Makimoto, T., "An aluminium nitride light-emitting diode with a wavelength of 210[thinsp]nanometres," Nature, 441(7091), 325-328 (2006).

[9] Guo, Q. X., Yoshitugu, M., Tanaka, T. *et al.*, "Microscopic investigations of aluminum nitride thin films grown by low-temperature reactive sputtering," Thin Solid Films, 483(1-2), 16-20 (2005).

[10] Li, K., Jin, H., Wang, D. M. *et al.*, "Preparation of AlN thin films for film bulk acoustic resonator application by radio frequency sputtering," Journal of Zhejiang University-Science A, 10(3), 464-470 (2009).

[11] Xiong, J., Gu, H.-s., Hu, K. *et al.*, "Influence of substrate metals on the crystal growth of AlN films," International Journal of Minerals, Metallurgy, and Materials, 17(1), 98-103.
[12] Qi-Chu, Z., "Metal-AlN cermet solar selective coatings deposited by direct current magnetron sputtering technology," Journal of Physics D: Applied Physics, 31(4), 355 (1998).
[13] Aryasomayajula, A., Canovic, S., Bhat, D. *et al.*, "Transmission electron microscopy and X-ray diffraction analysis of alumina coating by alternate-current inverted magnetron-sputtering technique," Thin Solid Films, 516(2-4), 397-401 (2007).
[14] Demiryont, H., Thompson, L. R., and Collins, G. J., "Optical and electrical characterizations of laser-chemical-vapor-deposited aluminum oxynitride films," Journal of Applied Physics, 59(9), 3235-3240 (1986).
[15] Levin, I., and Brandon, D., "Metastable Alumina Polymorphs: Crystal Structures and Transition Sequences," Journal of the American Ceramic Society, 81(8), 1995-2012 (1998).
[16] Zhao, Z. W., Tay, B. K., Yu, G. Q. *et al.*, "Optical properties of aluminium oxide thin films prepared at room temperature by off-plane filtered cathodic vacuum arc system," Thin Solid Films, 447-448, 14-19 (2004).
[17] Segda, B. G., Jacquet, M., and Besse, J. P., "Elaboration, characterization and dielectric properties study of amorphous alumina thin films deposited by r.f. magnetron sputtering," Vacuum, 62(1), 27-38 (2001).
[18] Xiao, W., and Jiang, X., "Optical and mechanical properties of nanocrystalline aluminum oxynitride films prepared by electron cyclotron resonance plasma enhanced chemical vapor deposition," Journal of Crystal Growth, 264(1-3), 165-171 (2004).
[19] Hartnett, T. M., Bernstein, S. D., Maguire, E. A. *et al.*, "Optical properties of ALON (aluminum oxynitride)," Infrared Physics & Technology, 39(4), 203-211 (1998).
[20] Wang, X., Li, W., and Seetharaman, S., "Thermodynamic study and synthesis of γ-aluminum oxynitride," Scandinavian Journal of Metallurgy, 31(1), 1-6 (2002).
[21] Barradas, N. P., Jeynes, C., and Webb, R. P., "Simulated annealing analysis of Rutherford backscattering data," Applied Physics Letters, 71(2), 291-293 (1997).
[22] Downs, R. T., Bartelmehs, K. L., Gibbs, G. V. *et al.*, "INTERACTIVE SOFTWARE FOR CALCULATING AND DISPLAYING X-RAY OR NEUTRON POWDER DIFFRACTOMETER PATTERNS OF CRYSTALLINE MATERIALS," American Mineralogist, 78(9-10), 1104-1107 (1993).
[23] Petrov, I, Barna *et al.*, "Microstructural evolution during film growth," American Institute of Physics, Melville, NY, ETATS-UNIS(2003).
[24] Borges, J., Vaz, F., and Marques, L., "AlNxOy thin films deposited by DC reactive magnetron sputtering," Applied Surface Science, 257(5), 1478-1483 (2010).
[25] Dirk Poelman and Philippe Frederic, S., "Methods for the determination of the optical constants of thin films from single transmission measurements: a critical review," Journal of Physics D: Applied Physics, 36(15), 1850 (2003).